

Directional adhesion of gecko-inspired angled microfiber arrays

Jongho Lee,¹ Ronald S. Fearing,² and Kyriakos Komvopoulos^{1,a)}

¹Department of Mechanical Engineering, University of California, Berkeley, California 94720, USA

²Department of Electrical Engineering and Computer Sciences, University of California, Berkeley, California 94720, USA

(Received 3 August 2008; accepted 2 October 2008; published online 13 November 2008)

Arrays of angled microfibers with a gecko-inspired structure were fabricated from a stiff thermoplastic polymer (polypropylene) with elastic properties similar to those of β -keratin of natural setae. Friction experiments demonstrated that this fibrillar polymer surface exhibits directional adhesion. Sliding of clean glass surfaces against and along the microfiber direction without applying an external normal force produced an apparent shear stress of 0.1 and 4.5 N/cm², respectively. This directional adhesion is interpreted in the context of a nonlinear elastic bending model of an angled beam. Shearing and normal contact experiments yielded further evidence of the anisotropic adhesion of the fibrillar polymer and revealed the occurrence of a pull-off (adhesive) force at the instant of surface detachment, unlike vertically aligned microfiber arrays of the same material that exhibited a zero pull-off force. The results of this study provide impetus for the design of gecko-inspired adhesives with angled structures that demonstrate directional adhesion against different material surfaces. © 2008 American Institute of Physics. [DOI: 10.1063/1.3006334]

Angled natural gecko setal arrays consisting of β -keratin (elastic modulus $E=1.5$ GPa)^{1,2} are characterized by a high normal compliance,² which is a key factor in producing high adhesion and directional properties, such as pure adhesion and high friction when sliding occurs along and against the setal direction, respectively.³ The unique directional properties of these hard-material-based angled setal arrays provide controllable^{3,4} and self-cleaning⁵ adhesion, enabling geckos to run up vertical walls as fast as 1 m/s.⁴

Angled microfibers are of critical importance in the design of geckolike surfaces with adjustable adhesion properties.⁶ Significant effort has been devoted to fabricate angled stalk arrays showing adhesion behaviors similar to those of gecko setae. For example, Santos *et al.*⁷ designed angled point-stalks of polyurethane ($E\approx 0.3$ MPa), Aksak *et al.*⁸ and Murphy *et al.*⁹ fabricated angled fiber arrays with and without spatula tips consisting of two different types of polyurethane ($E\approx 2.9$ and 9.8 MPa), and Yao *et al.*¹⁰ examined the properties of a thin-film layer deposited on tilted stalks of polydimethylsiloxane ($E\approx 3$ MPa). These structures demonstrate directional properties characteristic of gecko-inspired synthetic adhesives.¹¹ However, angled fibrillar adhesives consisting of a hard polymer that exhibit anisotropic properties have not been fabricated yet.

Since hard polymers do not generate significant adhesion even down to the millimeter scale, they are promising materials for gecko-inspired synthetic adhesives demonstrating high durability and self-cleaning capability.⁵ Therefore, the main objective of this study was to investigate whether gecko-inspired adhesives consisting of angled microfiber arrays can be fabricated from a hard polymer with mechanical properties similar to those of β -keratin of natural setae, such as polypropylene.

Vertically aligned arrays of high-density microfibers were fabricated by a molding method described elsewhere.¹² Tensile tests (Sintech tensile tester 2/S, MTS Systems) re-

vealed a polypropylene elastic modulus of ~ 1.5 GPa. The vertically aligned microfiber array patch was covered by a 25- μm -thick polyimide film placed on a clean microscope glass slide (Fisher Scientific), and the stack was processed by rollers (Catena 35, General Binding Corporation) that were heated at 50 °C [Fig. 1(a)] to form angled microfiber arrays [Fig. 1(b)]. Scanning electron microscope (SEM) images of top and side views of fabricated angled microfiber arrays are shown in Figs. 1(c) and 1(d), respectively. The average tilt angle of the unloaded microfibers from the surface normal is $\theta_0=45^\circ$ and the average center-to-center microfiber distance is equal to 1.5 μm .

The directional adhesion behavior of 2×2 cm² samples was examined with a custom-made one-axis force sensor¹² that measures the shear force F_s due to sliding a microfiber array against a substrate without applying a normal force F_n . Before each test, the angled microfiber array was placed on a glass substrate cleaned with isopropanol and a normal force

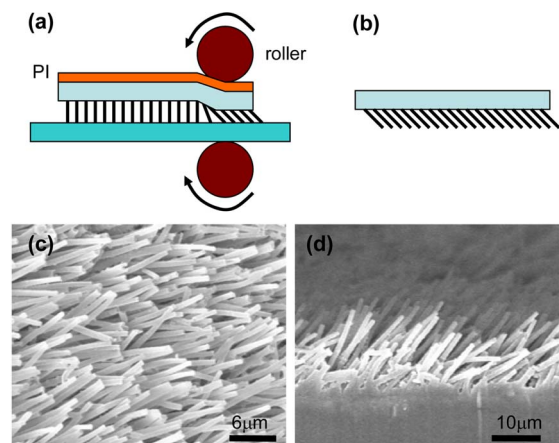


FIG. 1. (Color online) Schematic illustration of the fabrication process of angled microfiber arrays and SEM images of the produced fibrillar adhesive. (a) A vertically aligned microfiber array is passed between rollers heated at 50 °C, while a polyimide (PI) film prevents sample adhesion to the hot rollers. (b) The resulting synthetic fibrillar adhesive consists of an angled microfiber array. (c) Top and (d) side views of the angled fibrillar adhesive.

^{a)}Author to whom correspondence should be addressed. Electronic mail: kyriakos@me.berkeley.edu.

was applied to generate an apparent compressive stress of ≤ 0.1 N/cm². Then, the normal force was removed and the entire stage, including the glass substrate, was displaced laterally either along or against the microfiber direction at a constant speed of 120 μ m/s. Although testing was performed under a zero external normal force, a very small compressive stress of ~ 0.5 mN/cm² due to the sample weight was applied to the microfibers. The estimated microfiber contact area was determined from *in-situ* observations obtained with a camera, using frustrated total internal reflection at the interface of the side-illuminated glass substrate and the microfiber array.^{12,13} It is assumed that all of the microfibers in the estimated microfiber contact area are in contact with the glass substrate.

In addition to the tests with the one-axis force sensor, experiments were also performed with a two-axis force sensor to further examine the directional adhesion of the fibrillar adhesive and the development of a pull-off (adhesive) force at the instant of surface separation after pure normal loading. Instead of a spherical indenter used in earlier studies,¹⁴ a 2×5 mm² sample was attached to a flat glass indenter by cyanoacrylate instant adhesive (495, Loctite) and aligned coplanar with a clean glass substrate using a high-magnification lens (Edmund Scientific) and a viewing camera (MicroPublisher 5.0 RTV, QImaging). In all of the sliding tests with the two-axis force transducer, the sliding speed was fixed at 10 μ m/s.

The evolution of the shear force due to sliding along and against the microfiber direction in the absence of an external normal force is shown in Fig. 2(a). The plot contains two types of results: (a) statistical results, i.e., mean (solid curve) and standard deviation (error bars) shear force data obtained from seven tests, in which sliding occurred along the microfiber direction, and (b) typical shear force responses due to sequential sliding along and against the microfiber direction (discontinuous curves 1–4). Sliding along the microfiber direction enhanced the sample engagement, leading to an increase in the shear force (curve 1). This trend is attributed to the continuously increased contribution of adhesion to the shear force needed to maintain sliding, caused by the increase in the real contact area with the surface conformity as a result of microfiber bending. Although subsequent sliding against the microfiber direction produced a very small shear force (curve 2), sliding again along the microfiber direction yielded an increase in shear force (curve 3) similar to that observed initially (curve 1). Finally, sliding against the microfiber direction yielded again a shear force close to zero (curve 4), illustrating repeatable directional adhesion.

The mean shear force due to sliding along the microfiber direction [solid curve, Fig. 2(a)] consists of three regimes. The zero shear force up to ~ 8 s from the onset of sliding (first regime) is due to the slack string connected to the force sensor that inhibited microfiber slip. The subsequent increase in the shear force (second regime) represents a transient period in which continuous bending of contacting microfibers resulted in more microfiber contact that increased the real contact area and, in turn, the shear force to maintain sliding. Equilibrium was reached at the microfiber/glass interface after sliding for ~ 60 s along the microfiber direction, resulting in a steady-state shear force of 8–10 N (third regime).

The directional dependence of the shear force [Fig. 2(a)] can be interpreted in the context of an elastic bending model of an angled beam. Previous analyses provided insight into

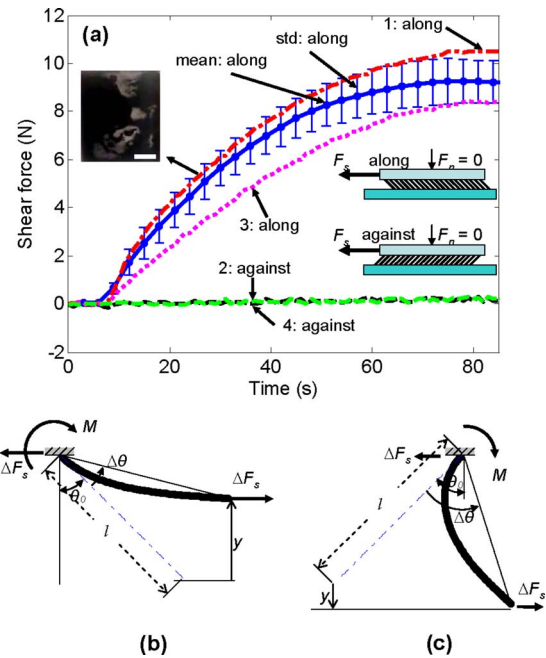


FIG. 2. (Color online) (a) Evolution of shear force of angled fibrillar adhesive during sliding in the absence of an external normal force. Average (solid line) and standard deviation (error bars) data were obtained from seven tests in which sliding occurred along the microfiber direction. The testing sequence in the multiple-sliding experiment was along (dash-dot line 1), against (dash line 2), along (dot line 3) and, finally, against (dash line 4) the microfiber direction. The inset shows an optical image of contact regions (bright spots) used to estimate the microfiber contact area for sliding along the microfiber direction (scale bar=5 mm). Schematics of an angled microfiber undergoing bending due to sliding (b) along and (c) against the microfiber direction in the absence of an external normal force.

the dependence of the contact force at a fiber tip on the fiber angle and sliding direction,⁶ and the variation in the normal force at a flat tip with the fiber angle and deflection.⁸ Since the normal pressure due to the sample weight can be ignored as negligibly small, the angle $\theta(s)$ from the surface normal due to a shear force applied at the free end of a microfiber ΔF_s [Figs. 2(b) and 2(c)], where s is the distance from the fixed end of the beam, is the solution of the following differential equation derived from elastic beam theory:

$$EI \frac{d^2 \theta}{ds^2} + \Delta F_s \cos \theta = 0, \quad (1)$$

where $I(=\pi r^4/4)$ is the moment of inertia, r is the microfiber radius, $\theta(=\theta_0 + \Delta\theta)$ is the angle from the surface normal, and $\Delta\theta$ is the deviation angle from θ_0 due to the shear force ΔF_s .

The microfiber density n of the fibrillar adhesive [Fig. 1(b)] is equal to the filter pore density (42×10^6 pores/cm²). For steady-state sliding along the microfiber direction (i.e., $F_s \approx 9$ N), the estimated microfiber contact area A , determined from seven tests (image processing toolbox, Matlab, Mathworks), was found equal to 0.18 (± 0.02) times the apparent contact area (4 cm²). Hence, the steady-state shear force per microfiber ($\Delta F_s = F_s/nA$) due to sliding along the microfiber direction [Fig. 2(b)] is estimated to be $\Delta F_s \approx 298$ nN. For $l=18$ μ m, $r=0.3$ μ m, $E=1.5$ GPa, and $\Delta F_s=298$ nN and boundary conditions $\theta(0)=45^\circ$ and $M(l)=0$, numerical integration of Eq. (1) (Matlab, Mathworks) yields $\Delta\theta=31^\circ$ [Fig. 2(b)]. Thus, the increase in the shear force to a steady-state of ~ 9 N [solid curve, Fig. 2(a)] is attributed to the increase in the real con-

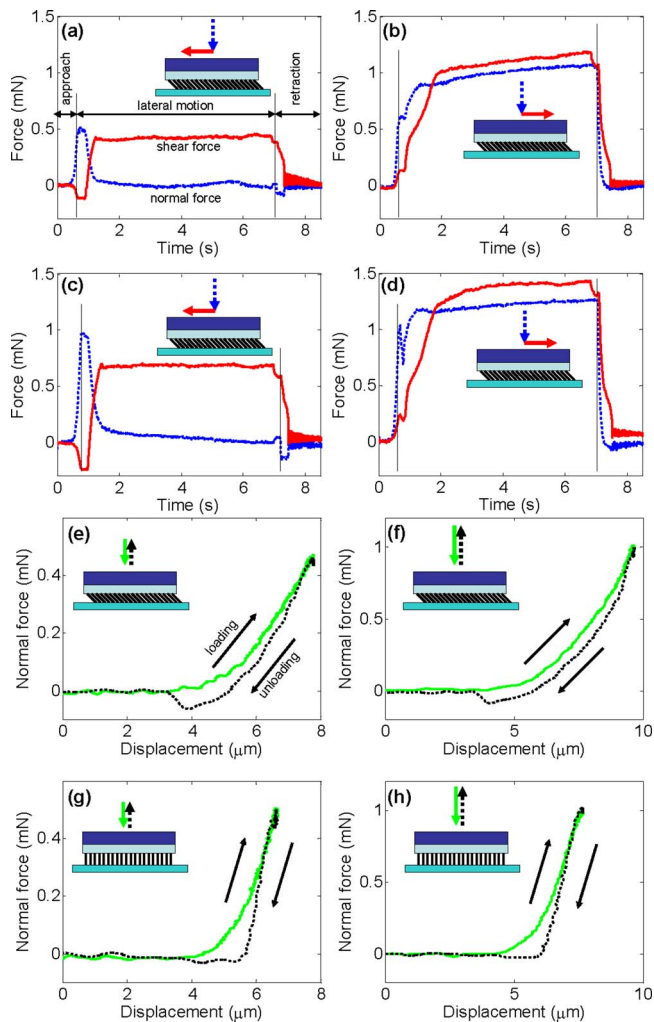


FIG. 3. (Color online) Shear force responses of angled microfiber arrays for sliding [(a) and (c)] along and [(b) and (d)] against the microfiber direction under a fixed normal displacement produced by applying a normal force (preload) of 0.5 and 1 mN, and normal force vs displacement responses of [(e) and (f)] angled and [(g) and (h)] vertically aligned microfiber arrays.

tact area due to microfiber bending that increased the number of microfibers in contact with the substrate and, in turn, the contribution of adhesion to the total shear force. For sliding against the microfiber direction, $F_s \approx 0.2$ N [e.g., curves 2 and 4 in Fig. 2(a)] and A is ~ 0.01 times the apparent area (observed *in situ* as described earlier). Thus, the estimated steady-state shear force is $\Delta F_s \approx 119$ nN. For boundary conditions $\theta(0) = -45^\circ$ and $M(l) = 0$, numerical integration of Eq. (1) yields $\Delta\theta = 71^\circ$. Thus, sliding along the microfiber direction produced a much higher shear force (by a factor of 2.5) and less bending than sliding against the microfiber direction. From the numerical solution, the backing-substrate distance was predicted to decrease by $y = 8.4$ μm [Fig. 2(b)]. Since this gap decrease is much larger than the microfiber height variation (~ 3 μm), a significant increase in the number of contacting microfibers (or real contact area) is predicted for sliding along the microfiber direction. Alternatively, an increase in the backing-substrate gap by $y = 2.5$ μm [Fig. 2(c)] was calculated for sliding against the microfiber direction, suggesting that even microfibers initially in contact with the glass substrate were detached during sliding, resulting in a significant decrease in the real contact area and, in turn, negligibly small shear force. These

arguments are in agreement with experimental measurements of the estimated microfiber contact area for sliding along (0.72 cm^2) and against (0.04 cm^2) the microfiber direction.

Figure 3 shows shear and normal force responses of angled and vertical microfiber arrays obtained from sliding (under a fixed normal displacement) and pure normal contact experiments performed with a displacement-controlled two-axis stage. As shown in Figs. 3(a) and 3(c), sliding along the microfiber direction, while maintaining the normal displacement that produced a normal force (preload) $F_n = 0.5$ and 1.0 mN, respectively, resulted in pure shear loading throughout most of the test duration. The negative shear force during preloading is attributed to the force applied to the flat indenter by the compressed microfibers. Surface separation at the end of sliding produced a small tensile (negative) normal force. A markedly different behavior was observed when sliding occurred against the microfiber direction under identical preloads. As evidenced from Figs. 3(b) and 3(d), a marked increase in the shear force and a high normal force were produced in this case, resulting in a high coefficient of friction of 1.1. Furthermore, a negative (tensile) normal force was not observed at the instant of surface separation. Therefore, even at the millimeter scale, the angled microfiber array demonstrated pure adhesion in one direction and high sliding friction in the opposite direction. In addition, an adhesive pull-off force was measured at the instant of surface separation of the angled microfiber array [Figs. 3(e) and 3(f)], as opposed to the vertically aligned microfiber array that produced a virtually zero pull-off force [Figs. 3(g) and 3(h)].

In conclusion, gecko-inspired angled fibrillar adhesives fabricated from a hard polymer (polypropylene) demonstrated pure adhesion in one direction and high sliding friction in the opposite direction, similar to gecko setal arrays. The anisotropic adhesion of the angled microfiber arrays was interpreted in the context of a nonlinear elastic bending model of an angled beam. A significant pull-off force was observed at the instant of surface separation of the angled microfiber array after pure normal contact, indicative of its higher compliance (hence, higher adhesion) compared to arrays of vertically aligned microfibers.

- ¹A. M. Peattie, C. Majidi, A. Corder, and R. J. Full, *J. R. Soc., Interface* **4**, 1071 (2007).
- ²K. Autumn, C. Majidi, R. E. Groff, A. Dittmore, and R. Fearing, *J. Exp. Biol.* **209**, 3558 (2006).
- ³K. Autumn, A. Dittmore, D. Santos, M. Spenko, and M. Cutkosky, *J. Exp. Biol.* **209**, 3569 (2006).
- ⁴N. Gravish, M. Wilkinson, and K. Autumn, *J. R. Soc., Interface* **5**, 339 (2008).
- ⁵W. R. Hansen and K. Autumn, *Proc. Natl. Acad. Sci. U.S.A.* **102**, 385 (2005).
- ⁶M. Sitti and R. S. Fearing, *J. Adhes. Sci. Technol.* **17**, 1055 (2003).
- ⁷D. Santos, M. Spenko, A. Parness, S. Kim, and M. Cutkosky, *J. Adhes. Sci. Technol.* **21**, 1317 (2007).
- ⁸B. Aksak, M. P. Murphy, and M. Sitti, *Langmuir* **23**, 3322 (2007).
- ⁹M. P. Murphy, B. Aksak, and M. Sitti, *J. Adhes. Sci. Technol.* **21**, 1281 (2007).
- ¹⁰H. Yao, G. D. Rocca, P. R. Guduru, and H. Gao, *J. R. Soc., Interface* **5**, 723 (2008).
- ¹¹K. Autumn and N. Gravish, *Philos. Trans. R. Soc. London, Ser. A* **366**, 1575 (2008).
- ¹²J. Lee, C. Majidi, B. Schubert, and R. S. Fearing, *J. R. Soc., Interface* **5**, 835 (2008).
- ¹³S. Begej, *IEEE J. Rob. Autom.* **4**, 472 (1988).
- ¹⁴B. Schubert, J. Lee, C. Majidi, and R. S. Fearing, *J. R. Soc., Interface* **5**, 845 (2008).